

Power-Law Slip Profile of the Moving Contact Line in Two-Phase Immiscible Flows

Tiezheng Qian,¹ Xiao-Ping Wang,¹ and Ping Sheng²

¹*Department of Mathematics, Hong Kong University of Science and Technology, Clear Water Bay, Kowloon, Hong Kong, China*

²*Department of Physics and Institute of Nano Science and Technology, Hong Kong University of Science and Technology, Clear Water Bay, Kowloon, Hong Kong, China*

(Received 28 October 2003; published 27 August 2004)

Large-scale molecular dynamics (MD) simulations on two-phase immiscible flows show that, associated with the moving contact line, there is a very large $1/x$ partial-slip region where x denotes the distance from the contact line. This power-law partial-slip region is verified in large-scale adaptive continuum calculations based on a local, continuum hydrodynamic formulation, which has proved successful in reproducing MD results at the nanoscale. Both MD simulations and numerical solutions of continuum equations indicate the existence of a universal slip profile in the Stokes-flow regime.

DOI: 10.1103/PhysRevLett.93.094501

PACS numbers: 47.11.+j, 68.08.-p, 83.10.Ff, 83.10.Mj

The no-slip condition, i.e., zero relative velocity between the fluid and the solid at the interface, has been the paradigm in most of the hydrodynamics literature [1]. In molecular dynamics (MD) simulations, however, a small amount of relative slip between the fluid and the solid surface is generally detected at a high flow rate [2]. Such a slip can be accounted for by the Navier boundary condition (NBC), whereby the slip velocity is proportional to the tangential viscous stress [2,3]. The proportionality constant between the slip velocity v^{slip} and the shear rate is denoted as the slip length l_s , usually ranging from one to a few nanometers (from MD simulations). As the amount of slip is extremely small in subsonic flow rates, the NBC is practically indistinguishable from the no-slip condition in most situations. In contrast, for immiscible flows the MD simulations have shown near-complete slip in the vicinity of the moving contact line (MCL), defined as the intersection of fluid-fluid interface with the solid wall [4–6]. An intriguing question ensues: In a mesoscopic or macroscopic system, what is the slip profile which consistently interpolates between the near-complete slip at the MCL and the no-slip boundary condition that must hold at regions far away [7,8]? Recent evidence has shown the slip profile obtained from nanoscale MD simulations to be accountable by the generalized Navier boundary condition (GNBC), in which the slip velocity is proportional to the total tangential stress—the sum of the viscous stress and the uncompensated Young stress; the latter arises from the deviation of the fluid-fluid interface from its static configuration [6]. Here we show through large-scale MD simulations and continuum hydrodynamic calculations that there exists a power-law partial-slip region extending to hundreds of nanometers or even more, contrary to the usual expectation of a nanometer-scale slip region in the vicinity of the MCL. The existence of this large partial-slip region modifies the conventional picture that significant NBC slipping occurs only under high flow/shear rate. Instead,

the power-law slip region is associated with the universal slip profile of the MCL, even at low flow rates.

MD simulations have been carried out for increasingly larger systems of immiscible Couette flow (Fig. 1). Two immiscible fluids were confined between two parallel walls in the xy plane, with the fluid-solid boundaries defined by $z = 0, H$. Periodic boundary conditions were imposed along the x and y directions. Interaction between fluid molecules separated by a distance r was modeled by a modified Lennard-Jones (LJ) potential $U_{ff} = 4\epsilon[(\sigma/r)^{12} - \delta_{ff}(\sigma/r)^6]$, where $\delta_{ff} = 1$ for like molecules and $\delta_{ff} = -1$ for molecules of different species. The average number density for the fluids was set at $\rho = 0.81/\sigma^3$. The temperature was controlled at $2.8\epsilon/k_B$, above the liquid-gas coexistence region. Each wall was constructed by two [001] planes of an fcc lattice, with each wall molecule attached to a lattice site by a harmonic spring. The mass of the wall molecule was set equal to that of the fluid molecule m . The number density

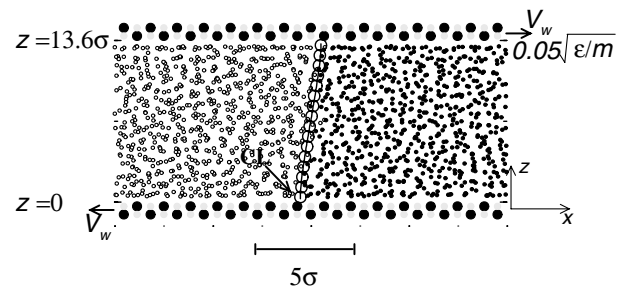


FIG. 1. Segment of the MD simulation sample for an immiscible Couette flow with a 90° static contact angle. The small empty and solid circles indicate the instantaneous molecular positions of the two fluids projected onto the xz plane. The horizontally aligned black and gray circles denote the wall molecules. Between the two fluids, the large hollow circles represent the time-averaged interface profile, defined by $\rho_1 = \rho_2$ ($\phi = 0$). The solid line is the interface profile calculated from the continuum hydrodynamic model.

of the wall was set at $\rho_w = 1.86/\sigma^3$. The wall-fluid interaction was modeled by another LJ potential U_{wf} with the energy and range parameters given by $\epsilon_{wf} = 1.16\epsilon$ and $\sigma_{wf} = 1.04\sigma$, and δ_{wf} for specifying the wetting property of the fluid, taken to be 1 in our simulations. The Couette flow was generated by moving the top and bottom walls at a constant speed V_w in the $\pm x$ directions, respectively. There is no locked layer of fluid molecules at the solid surface. In most of our simulations, the shearing speed was $V_w = 0.05\sqrt{\epsilon/m}$, the sample dimension along y was 6.8σ , the wall separation along z varied from $H = 6.8\sigma$ to 68σ , and the sample dimension along x was set to be long enough so that the uniform single-phase shear flow was recovered far away from the MCL. Steady-state interfacial and velocity profiles were obtained from time average over $5 \times 10^5\tau$ where τ is the atomic time scale $\sqrt{m\sigma^2/\epsilon}$.

The tangential slip velocity profiles next to the wall, i.e., the slip profiles, are shown in the inset of Fig. 2. While there is clearly a small core region, on the order of a few l_s , where the slip profiles display sharp decay, a much gentler variation of the slip profiles becomes apparent as the system size H increases. In order to quantify the nature of the gentle variation, we plot in Fig. 2 the same data in the log-log scale. The dashed line has a slope of -1 , indicating the $1/x$ behavior to be, indeed, realized in MD simulations. For our finite-sized systems, there is always a plateau in the slip velocity in each of the single-phase flows, also observable in MD simulations with a value given by $v_0^{\text{slip}} = 2V_w l_s / (H + 2l_s)$, which acts as an outer cutoff on the $1/x$ profile. This v_0^{slip} expression is simply derived from the Navier-Stokes equation for uniform shear flow and the NBC. From our largest MD simulation, the $v^{\text{slip}} \propto 1/x$ behavior is seen to extend to $\sim 50\sigma$ (or $\sim 25l_s$). Hence as $H \rightarrow \infty$ and v_0^{slip} approaches 0 (no slip), the power-law region can be very large indeed. A large $1/x$ partial-slip region is significant, because the outer cutoff length scale directly determines the integrated effects, such as the total steady-state dissipation. While in the past the $1/x$ stress variation away from the MCL has been known [9], to our knowledge the fact that the partial slip also exhibits the same spatial dependence has not been previously seen [10], even though the validity of the Navier boundary condition at high shear stress has been verified [2,3].

Since our MD simulations reach the capacity limit (e.g., for $V_w/\sqrt{\epsilon/m} \ll 1$) quickly, a continuum hydrodynamic formulation is necessary for realistic simulations. Combining the GNBC with the Cahn-Hilliard (CH) hydrodynamic formulation of two-phase flow [11–13], we have obtained a continuum hydrodynamic model [6] that is accurate to the molecular scale. The two coupled equations of motion are the Navier-Stokes equation (with the addition of the capillary force density) and the CH

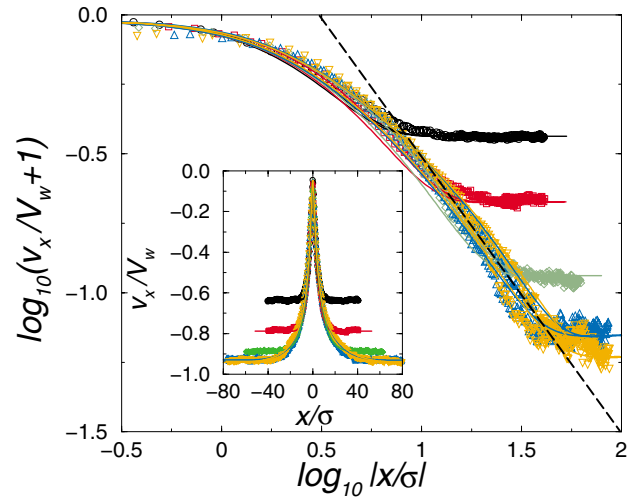


FIG. 2 (color). Log-log plot of the slip profiles showing the $1/x$ behavior. Here $v_x/V_w + 1$ is the scaled slip velocity at the lower fluid-solid interface $z = 0$, and x/σ measures the distance from the MCL in units of σ . The wall is moving at $-V_w$; hence $v_x/V_w = 0$ means complete slip and $v_x/V_w = -1$ means no slip. The v_x profiles were obtained for five symmetric cases of identical wall-fluid interactions for the two fluids (both $\delta_{wf} = 1$ and thus a 90° static contact angle). The five cases shown here used different values for H but the same value for V_w ($= 0.05\sqrt{\epsilon/m}$) and also the same parameters for densities and interactions. The symbols represent the MD results and the solid lines represent the continuum hydrodynamics results, obtained for $H = 6.8\sigma$ (black circles and line), $H = 13.6\sigma$ (red squares and line), $H = 27.2\sigma$ (green diamonds and line), $H = 54.4\sigma$ (blue up triangles and line), and $H = 68\sigma$ (orange down triangles and line). There are two solid curves for each color, one curve for the slip profile left to the MCL and the other for the slip profile right to the MCL. The dashed line has the slope of -1 , indicating that the $1/x$ behavior is approached for increasingly larger H . For $H = 68\sigma$, the $1/x$ behavior extends from $|x| \approx 12\sigma \approx 6l_s$ to $50\sigma \approx 25l_s$, where l_s was measured to be 2σ . Inset: The scaled tangential velocity v_x/V_w at $z = 0$ is plotted as a function of x/σ .

convection-diffusion equation for the composition field $\phi(\mathbf{r}) = (\rho_2 - \rho_1)/(\rho_2 + \rho_1)$ (where ρ_1 and ρ_2 are the local number densities for the two fluid species):

$$m\rho \left[\frac{\partial \mathbf{v}}{\partial t} + (\mathbf{v} \cdot \nabla) \mathbf{v} \right] = -\nabla p + \nabla \cdot \boldsymbol{\sigma}^v + \mu \nabla \phi + m\rho \mathbf{g}_{\text{ext}}, \quad (1a)$$

$$\partial \phi / \partial t + \mathbf{v} \cdot \nabla \phi = M \nabla^2 \mu, \quad (1b)$$

together with the incompressibility condition $\nabla \cdot \mathbf{v} = 0$. Here $m\rho$ is the average fluid mass density, p is the pressure, $\boldsymbol{\sigma}^v$ is the Newtonian viscous stress tensor, $\mu \nabla \phi$ is the capillary force density with $\mu = \delta F / \delta \phi$ being the chemical potential defined from the CH free energy functional F [14], $m\rho \mathbf{g}_{\text{ext}}$ is the external body force density (for Poiseuille flows), and M is the phe-

nomenological mobility coefficient. The boundary conditions at the solid surface are $v_n = 0$, $\partial_n \mu = 0$ (n denotes the outward surface normal), the continuum form of the GNBC:

$$\beta v_x^{\text{slip}} = -\eta \partial_n v_x + L(\phi) \partial_x \phi, \quad (1c)$$

and the relaxational equation for surface ϕ :

$$\partial \phi / \partial t + \mathbf{v} \cdot \nabla \phi = -\Gamma L(\phi). \quad (1d)$$

Here $L(\phi) = K \partial_n \phi + \partial \gamma_{wf}(\phi) / \partial \phi$ with $\gamma_{wf}(\phi)$ being the wall-fluid interfacial free energy density, $L(\phi) \partial_x \phi$ is the uncompensated Young stress, and Γ is a (positive) phenomenological parameter.

The continuum results shown in Fig. 2 were calculated on a uniform mesh, using the same set of material parameters and M , Γ values corresponding to the same local properties in all the five MD simulations [6]. The overall agreement is excellent. Such agreement is possible because the GNBC does not impose an artificial cutoff on the slip region. Below we extend the MCL simulations, through continuum hydrodynamics, to lower flow rates and much larger systems.

The continuum calculation for macroscopic immiscible flows is a challenging task. Methods based on a fixed uniform mesh would break down because it cannot afford to simulate macroscopic systems with molecular resolution near the MCL. We have employed for this problem the adaptive method based on iterative grid redistribution [15]. The computational mesh is redistributed according to the behavior of the continuum solution so that fine molecular resolution is achieved in the interfacial region and near the MCL, while elsewhere a much coarser mesh is used to save computational cost [6]. A semi-implicit time stepping scheme is also used to speed up the approach to steady state.

Figure 3 shows the continuum results for three large systems (H on the order of hundreds of σ) with small V_w ($\sim 0.001\sqrt{\epsilon/m}$, well beyond the capacity of our MD simulations). In all three cases, the capillary force was verified to be important only in the interfacial region. However, the pressure gradients and viscous forces shows a much slower variation. They are balanced outside the interfacial region, indicating the flow to be governed by the Stokes equation. This is expected, because the Reynolds number $m\rho V_w H / \eta \approx 0.6$ for $\rho \approx 0.8/\sigma^3$, $V_w = 0.005\sqrt{\epsilon/m}$, $H \approx 300\sigma$, and $\eta \approx 2.0\sqrt{\epsilon m}/\sigma^2$. In Fig. 3 the slip profiles, plotted on the log-log scale, clearly show the $1/x$ behavior extending from $|x| \approx 6l_s$ to $|x| \approx 270l_s$. The inset of Fig. 3 shows the scaled tangential velocity profiles at the solid surface, from which the existence of universal slip profile is evident. Physically, when $H \gg l_s$, the regime of Stokes flow is governed by only one velocity scale V_w and one length scale l_s . Thus universality becomes evident in terms of v_x/V_w plotted as a function of x/l_s .

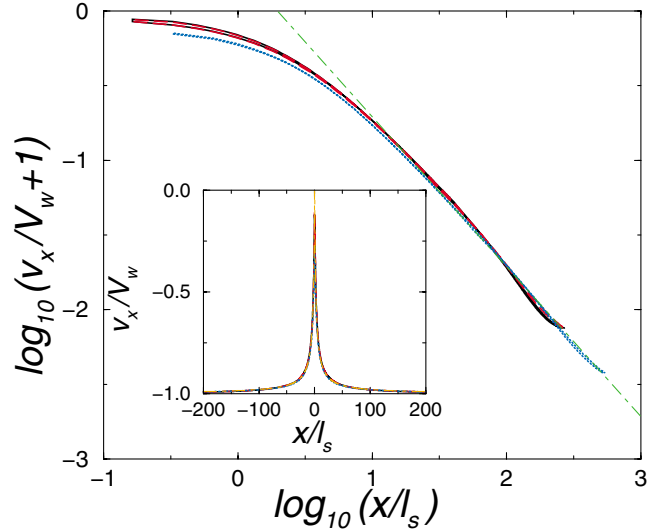


FIG. 3 (color). Log-log plot of the slip profiles showing the $1/x$ behavior. Here $v_x/V_w + 1$ is the scaled slip velocity at the lower fluid-solid interface $z = 0$, and x/l_s measures the distance from the MCL in units of l_s . The wall is moving at $-V_w$; hence $v_x/V_w = 0$ means complete slip and $v_x/V_w = -1$ means no slip. The black solid line denotes the case of $H = 326\sigma$, $V_w = 0.005\sqrt{\epsilon/m}$, and $l_s = 1.24\sigma$, the red dashed line denotes the case of $H = 326\sigma$, $V_w = 0.0025\sqrt{\epsilon/m}$, and $l_s = 1.24\sigma$, and the blue dotted line denotes the case of $H = 326\sigma$, $V_w = 0.0025\sqrt{\epsilon/m}$, and $l_s = 0.62\sigma$. The green dot-dashed line has the slope of -1 , indicating a power-law region much wider than that in Fig. 2. Inset: Universal slip profile. The scaled tangential velocities v_x/V_w at $z = 0$ for all three cases are plotted as a function of the scaled coordinate x/l_s . It is seen that the slip profiles show a partial-slip region as large as hundreds of l_s . The relation $v_x/V_w = 1/(1 + |x|/2.14l_s) - 1$ is also plotted by the orange dot-dashed line, showing an extremely good fit.

(The inset of Fig. 2 has already shown part of the universality, that the core slip profile is independent of the system size H .) A heuristic account of the universal slip profile is as follows. Away from the MCL, the viscous shear stress is given by $-a\eta v_x(x)/|x|$, where a is a constant ~ 1 , η the viscosity, and $v_x(x)$ the local tangential velocity. The NBC implies $v_x^{\text{slip}}(x) = -l_s a v_x(x)/|x|$. Since $v_x^{\text{slip}}(x) = v_x + V_w$, combining the two equations yields $v_x^{\text{slip}}(x)/V_w = 1/(1 + |x|/al_s)$ [16]. This relation, with $a \approx 2.14$ for best fit, agrees with the continuum slip profiles extremely well, as seen in the inset of Fig. 3.

In the Couette geometry, external work is supplied to maintain the constant speed V_w of the moving wall. The rate of work is given by the integral of the local tangential force $l_s^{-1}\eta|v^{\text{slip}}|$ times the wall speed V_w [6], i.e., $\int (l_s^{-1}\eta|v^{\text{slip}}|)V_w dx = \eta V_w^2 \mathcal{A}$ per unit length along y , where \mathcal{A} is a numerical constant. In the limit $V_w \rightarrow 0$ and $l_s/H \rightarrow 0$, \mathcal{A} is independent of V_w and l_s but depends on the outer cutoff of the $1/x$ profile. As the external work

done in the steady state must be fully dissipated, the total dissipation rate is equal to the rate of external work.

Slip profiles obtained from both MD simulations and numerical solutions of continuum equations show that the $1/x$ partial-slip region starts from $x_c \approx 6l_s$ ($v^{\text{slip}} \approx 0.26V_w$). The outer cutoff for the partial-slip region, denoted by R , is determined by the overall size of the system. For the total dissipation, the contributions of the core region and the partial-slip region may be quantified by the dimensionless integrations

$$\mathcal{A} = C = \int_0^{x_c} \left[\frac{|v^{\text{slip}}(x)|}{V_w} \right] d\left(\frac{x}{l_s}\right) \approx 2.9$$

for the core and

$$\mathcal{A} = \mathcal{P} = \int_{x_c}^R \left[\frac{|v^{\text{slip}}(x)|}{V_w} \right] d\left(\frac{x}{l_s}\right) \approx 2.14 \ln \frac{2.14 + R/l_s}{2.14 + x_c/l_s},$$

for the $1/x$ region. Assuming $l_s \sim 1$ nm (a few σ 's) [2], for $x_c = 10$ nm and $R = 1$ μm we have $\mathcal{P} \approx 9.2$, while for $x_c = 10$ nm and $R = 1$ mm we have $\mathcal{P} \approx 24$; i.e., the power-law region can contribute significantly more to the total dissipation than the core region.

The dissipation component that occurs at the fluid-solid interface can be evaluated as $\int (l_s^{-1} \eta |v^{\text{slip}}|^2) dx = \eta V_w^2 I$ per unit length along y , where

$$I = \int_0^R \left[\frac{|v^{\text{slip}}(x)|}{V_w} \right]^2 d\left(\frac{x}{l_s}\right) \approx \frac{2.14R/l_s}{2.14 + R/l_s}.$$

In the core region, the interfacial component of the dissipation is obtained by letting $R = x_c$, or $I \approx 1.6$, i.e., about 70% of the total interfacial dissipation ($I = 2.14$ for $R/l_s \rightarrow \infty$).

Recently, there has been considerable interest in the transport at microscales and nanoscales. The lower limit for R can reach submicrometer or even shorter length scales. On the other hand, there has been increasing evidence for large slip length realized in various fluid-solid interfaces [17–19]. Slip length l_s as large as 1 μm has been reported [18,19]. The results in this Letter indicate that fluid-solid interfacial dissipation is an important contribution to the total dissipation if large slip length occurs in a small system. While asymptotic analysis has shown that at large distances from the MCL the flow field is not sensitive to the slip boundary condition [20], the (macroscopic) asymptotic region may not be attained given the small system size and/or the large slip length. In this regard, a continuum hydrodynamic formulation of the contact line motion is necessary for realistic simulations of fluid dynamics at microscales and nanoscales, as done in the present case.

Partial support from HKUST's EHIA funding and Hong Kong RGC Grants No. HKUST 6176/99P, No. 6143/01P, and No. 604803 is hereby acknowledged.

-
- [1] G. K. Batchelor, *An Introduction to Fluid Dynamics* (Cambridge University Press, Cambridge, 1991).
 - [2] P. A. Thompson and S. M. Troian, *Nature (London)* **389**, 360 (1997).
 - [3] M. Cieplak, J. Koplik, and J. R. Banavar, *Phys. Rev. Lett.* **86**, 803 (2001).
 - [4] J. Koplik, J. R. Banavar, and J. F. Willemsen, *Phys. Rev. Lett.* **60**, 1282 (1988); *Phys. Fluids A* **1**, 781 (1989).
 - [5] P. A. Thompson and M. O. Robbins, *Phys. Rev. Lett.* **63**, 766 (1989); P. A. Thompson, W. B. Brinckerhoff, and M. O. Robbins, *J. Adhes. Sci. Technol.* **7**, 535 (1993).
 - [6] T. Z. Qian, X. P. Wang, and P. Sheng, *Phys. Rev. E* **68**, 016306 (2003).
 - [7] E. B. Dussan V., *Annu. Rev. Fluid Mech.* **11**, 371 (1979).
 - [8] P. G. de Gennes, *Rev. Mod. Phys.* **57**, 827 (1985).
 - [9] H. K. Moffatt, *J. Fluid Mech.* **18**, 1 (1964); C. Hua and L. E. Scriven, *J. Colloid Interface Sci.* **35**, 85 (1971). The $1/x$ stress variation along the wall can be derived from similarity solutions for Stokes flow when a boundary velocity or stress is prescribed in the presence of a contact line or a geometric corner.
 - [10] For example, an exponential slip profile was used in fitting the MD results in Ref. [5].
 - [11] H. Y. Chen, D. Jasnow, and J. Vinals, *Phys. Rev. Lett.* **85**, 1686 (2000).
 - [12] D. Jacqmin, *J. Fluid Mech.* **402**, 57 (2000).
 - [13] Based on the Cahn-Hilliard hydrodynamic formulation of binary fluids, a lattice Boltzmann model has been developed. See A. J. Briant and J. M. Yeomans, *Phys. Rev. E* **69**, 031603 (2004).
 - [14] J. W. Cahn and J. E. Hilliard, *J. Chem. Phys.* **28**, 258 (1958). The CH free energy functional is given by $F[\phi] = \int d\mathbf{r} [K(\nabla\phi)^2/2 + f(\phi)]$, where $f(\phi) = -r\phi^2/2 + u\phi^4/4$, and K , r , u are parameters which can be determined in MD simulations by measuring the interface profile thickness $\xi = \sqrt{K/r}$, the interfacial tension $2\sqrt{2}r^2\xi/3u$, and the two homogeneous equilibrium phases $\pm\sqrt{r/u}$ ($= \pm 1$ in our case). For details see Sec. IV of Ref. [6].
 - [15] W. Ren and X. P. Wang, *J. Comput. Phys.* **159**, 246 (2000).
 - [16] The similarity solution with a prescribed boundary velocity [9] becomes the leading order solution in an asymptotic expansion in the slip length l_s , if the NBC is applied. The leading order stress variation is $a\eta V_w/|x|$. As a consequence, the leading order contribution to the slip velocity is $al_s V_w/|x|$ (for small $l_s/|x|$).
 - [17] J-L. Barrat and L. Bocquet, *Phys. Rev. Lett.* **82**, 4671 (1999).
 - [18] D. C. Tretheway and C. D. Meinhart, *Phys. Fluids* **14**, L9 (2002).
 - [19] L. Leger, *J. Phys. Condens. Matter* **15**, S19 (2003).
 - [20] E. B. Dussan V., *J. Fluid Mech.* **77**, 665 (1976).